

*Dedicated to Professor Bogdan C. Simionescu  
on the occasion of his 65<sup>th</sup> anniversary*

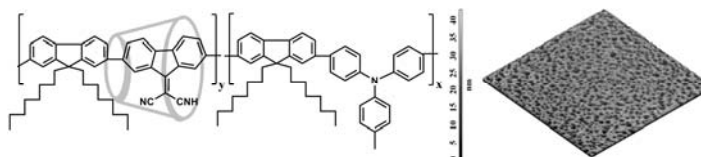
## SOME PHOTOPHYSICAL AND MORPHOLOGICAL PROPERTIES OF POLYROTAXANE BASED ON FLUORENE DERIVATIVES

Andreea STEFANACHE, Iuliana STOICA, Ana-Maria RESMERITA and Aurica FARCAS\*

“Petru Poni” Institute of Macromolecular Chemistry, 41A Grigore Ghica Vodă Alley, 700487 Iași, Roumania

Received October 2, 2012

Some photophysical and surface-morphological properties of fluorene polyrotaxane (PF<sub>r</sub>) prepared via Suzuki coupling from 9,9-dioctylfluorene-2,7-bis(trimethyleneborate) (1) with 4,4'-dibromo-4''-methyltriphenylamine (donor molecule) (2) and 2,7-dibromo-9-(dicyanomethylene) fluorene (acceptor molecule), as inclusion complex in  $\gamma$ CD (3c) in the feed molar ratios 50:35:15 and its PF non-rotaxane counterpart were investigated. These studies revealed an attractive approach to achieve desirable morphological and optical properties, as well as favourable solubility characteristics and film forming ability with higher uniformity, flatness, compared with the non-rotaxane PF ones. The AFM characterization presents a porous aspect with various pore sizes and two dimensional ordered structures of the polyrotaxane surface. Both copolymers showed blue-light emission in the film state.



### INTRODUCTION

Conjugated polymers have attracted much research interest over the past two decades due to their widespread applications in the field of materials science.<sup>1</sup> Among the various conjugated polymers, polyfluorene (PFs) and their derivatives have been extensively studied for the design of new molecular and polymeric materials because of their high photoluminescence quantum yields, their solubility and chemical stability, good film-forming ability and susceptibility to structural modification.<sup>2,3</sup> Nevertheless, there are some deficiencies that hamper their further applicability, firstly they show excimer and/or aggregate

formation upon thermal annealing or the passage of current and keto defect sites as a result of photo- or electro-oxidative degradation.<sup>4</sup> Another problem associated with PFs is the difference between electron and hole injection and transport, which greatly reduces the luminescence efficiency.<sup>5</sup> The main aspects that could be optimized from the point of view of their applications are high charge mobility along the individual polymer chains, a smooth morphology of the produced films, low band gap polymers and strong fluorescence efficiency. Not surprisingly, several approaches have been undertaken, in efforts to generate novel PFs, with enhanced device performance. The latest approach involves the copolymerization of the

\* Corresponding author: [afarcas@icmpp.ro](mailto:afarcas@icmpp.ro)

donor, with a higher HOMO (highest occupied molecular orbital), and the acceptor, with a lower LUMO (lowest occupied molecular orbital) energy level.<sup>6</sup> The high efficient light emitting diodes (LED) were obtained by incorporating of triarylamine derivatives (TA) as electron-donating into a multilayer device to balance the charge injection and transport.<sup>7</sup> It has been shown that the inclusion of the non-rigid structure of TA improves both high fluorescence efficiency in the solid state and high hole mobility. One the other hand, electron acceptors on the monomeric fluorenes (electron-deficient) have also received considerable attention in the study of electron-transport materials. Fluorene monomers with electron acceptors as dicyano groups at the C-9 position have gained special attraction, because have been found to be effective for tuning the band gaps of PFs,<sup>8</sup> and polyene with a 9-(dicyanomethylene) fluorene spacer with the lowest band gap of about 1.58 eV has been reported.<sup>9</sup> Among the various strategies the construction of mechanically interlocked molecules, such as rotaxanes and polyrotaxanes provide an example of supramolecular architectures, which attracted much interest during the past two decades, due to their possibility of insulating the backbones of conjugated polymers for controlling intermolecular interactions. In addition to that, there is the possibility of improving the solubility, fluorescence efficiency and morphological properties of the resulting polyrotaxanes.<sup>10-17</sup>

The current investigation continues our studies concerning the photophysical and morphological properties of polyrotaxanes with conjugated polymers. Herein, we report the effect of rotaxane formation on the preliminary photophysical and

morphological properties, as well as adhesion characteristics of randomly **PFc** fluorene polyrotaxane copolymer and compared them with the non-rotaxane **PF** reference samples. **PFc** and **PF** copolymers were obtained by Suzuki coupling approach starting from 9,9-dioctylfluorene-2,7-bis(trimethyleneborate) (**1**), 4,4'-dibromo-4''-methyltriphenylamine (**2**) (donor) and 2,7-dibromo-9-(dicyanomethylene) fluorene (acceptor) either in the form of its inclusion complex with  $\gamma$ -cyclodextrin (**3c**) or in non-complexed state (**3**) in the molar ratios 50:35:15 of **1** to **2** and **3c** or **3**.

## RESULTS AND DISCUSSION

The chemical structures of random **PFc** polyrotaxane copolymer and its corresponding **PF** non-rotaxane counterpart used in this study is depicted in Fig. 1.

To compare the effect of acceptor group content on the photophysical properties and morphological properties, **PFc** random polyrotaxane copolymer and its corresponding **PF** non-rotaxane counterpart were obtained by using Suzuki cross-coupling reaction of **1** to **2** (donor) and **3c** (complexed acceptor) or **3** (non-complexed acceptor) in the comonomer feed molar ratios of 50:35:15. By carrying out the coupling reaction in a 1/1 v/v mixture of DMF/toluene under N<sub>2</sub> at 100 °C temperature for 72 h, **PFc** rotaxane copolymer presented 53% coverage of acceptor structural units with  $\gamma$ CD, higher than in previously reported results.<sup>18</sup>

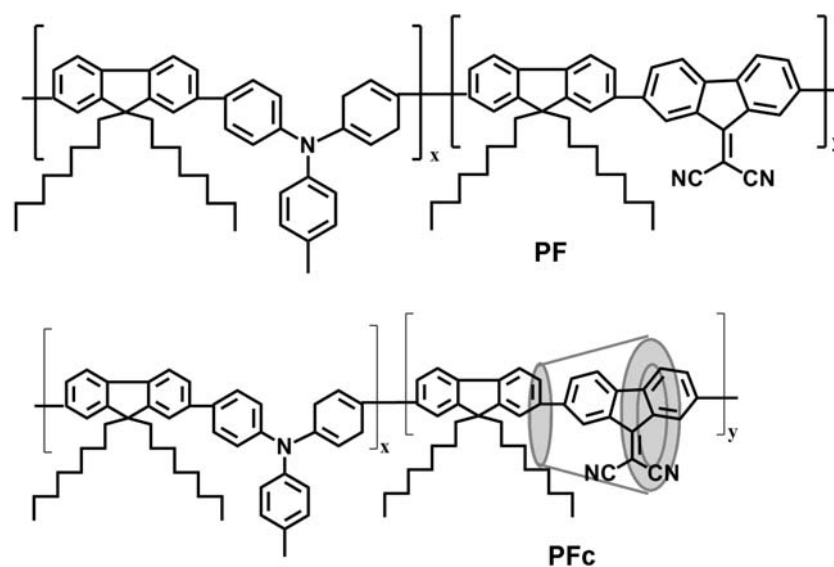


Fig. 1 – The chemical structures of **PF** and **PFc** copolymer samples.

The chemical structures of **PFc** and **PF** copolymers were confirmed by using FT-IR and NMR spectroscopy. FT-IR spectra of copolymers (not shown) reveal in each case the characteristic  $\nu(\text{CN})$  vibrational bands near  $2228\text{ cm}^{-1}$  in **PF**, while in **PFc** this band is shifted to  $2170\text{ cm}^{-1}$ . On the spectrum of **PFc** the vibration bands at  $3440\text{ cm}^{-1}$  (intensive and wide absorption band of O-H stretching vibration),  $1079\text{ cm}^{-1}$ , and  $1033\text{ cm}^{-1}$  (bands of ether bonds) indicated the presence of  $\gamma\text{CD}$ .

The  $^1\text{H}$  NMR spectra of **PFc** and **PF** copolymers were in good agreement with the proposed structures. Representative  $^1\text{H}$  NMR spectrum of **PFc** copolymer is shown in Fig. 2. The peaks at 8.05, 7.89 and 7.87 ppm are due the protons (labeled “c”, “b” and “a” in Fig. 2) from the acceptor molecule **3**. The multiple peaks in the range 6.83–7.77 ppm correspond to the other aromatic protons from the donor **2** and the comonomer **1** units. The resonance at 5.72, 5.67, 4.98, 4.97, 4.45, 4.42, 3.80, and 3.43 ppm are assigned to  $\gamma\text{CD}$ . The peaks at 2.17, 1.28, and 0.80 ppm correspond to the aliphatic protons in the octyl side chains. The NMR spectral analysis, was also used to determine the coverage of the rotaxane with macrocycle, *i.e.*, the average number of  $\gamma\text{CD}$  macrocycles per repeating unit, which has been calculated using the ratio of the integrated area of the peak assigned to the aromatic protons labeled

“c” in Fig. 2 (8.05 ppm,  $I_{\text{H}^c}$ ) and the anomeric H-1 proton of  $\gamma\text{CD}$  (4.98 ppm,  $I_{\text{H}^1}$ ),  $(I_{\text{H}^c}/2) / (I_{\text{H}^1}/8)$ . The average number of  $\gamma\text{CD}$  macrocycles per acceptor units, determined by  $^1\text{H}$  NMR in **PFc** copolymer structure has been found to be 0.53 (*i.e.*, 53% coverage).

To gain further insight into the effects of  $\gamma\text{CD}$  encapsulation, the UV-Vis absorption and fluorescence spectra of copolymers as thin films were performed. Their UV-Vis absorption spectra are shown in Fig. 3, and the spectroscopic analysis data are summarized in Table 1. The absorption UV-Vis spectra of **PF** and **PFc** showed a maximum at 385 nm, and 386 nm, respectively corresponding to the  $\pi\text{-}\pi^*$  transition of the polymer backbone (Fig. 3). The fluorescence emission of **PF** and **PFc** films reveals a blue emission with a maximum peak at 448 and 444 nm, respectively. Both absorption spectra of **PF** and **PFc** are red-shifted relative to those of previously reported copolymers (380 nm),<sup>18</sup> which can be understood as a result of increasing conjugation length and extended delocalization along the polymer backbone chain, upon inserting of higher content of acceptor units. Improved absorption intensity observed in **PFc** copolymer could be an indicative of a constructive excitonic coupling among the polymer chain, attributed to the protection of macrocycles.<sup>11,14</sup>

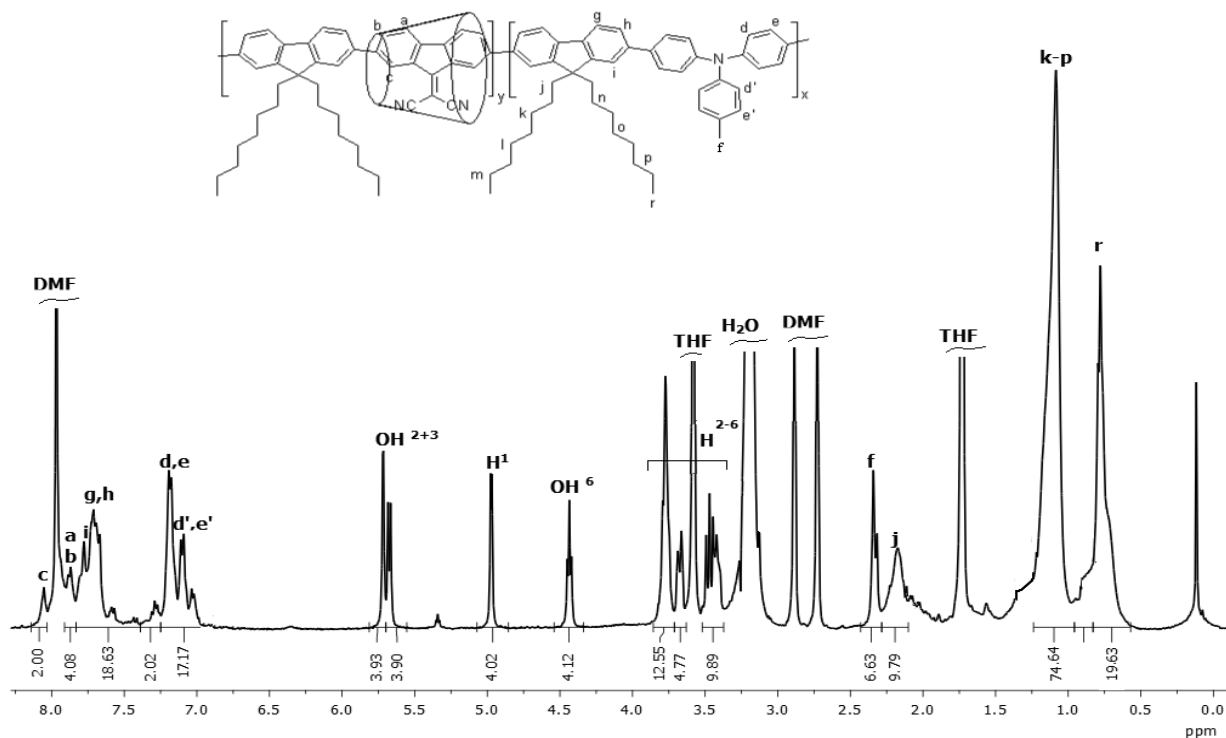


Fig. 2 –  $^1\text{H}$  NMR spectrum of **PFc** polyrotaxane in  $\text{THF-d}_8/\text{DMF-d}_7$ , 1/1 v/v.

Table 1

Optical properties of **PF** and **PFc** copolymers in solid state

Sample	Absorption $\lambda_{\max}^a$ (nm)	Emission $\lambda_{\max}^a$ (nm)
<b>PF</b>	385	448
<b>PFc</b>	386	444

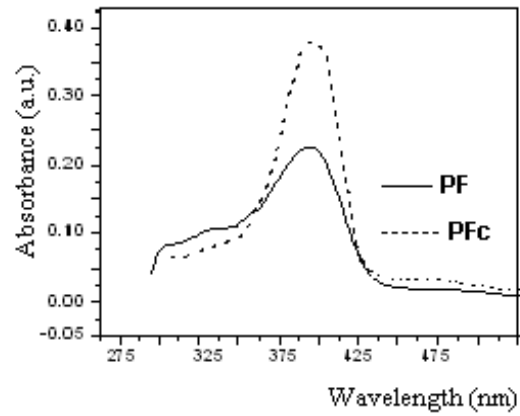
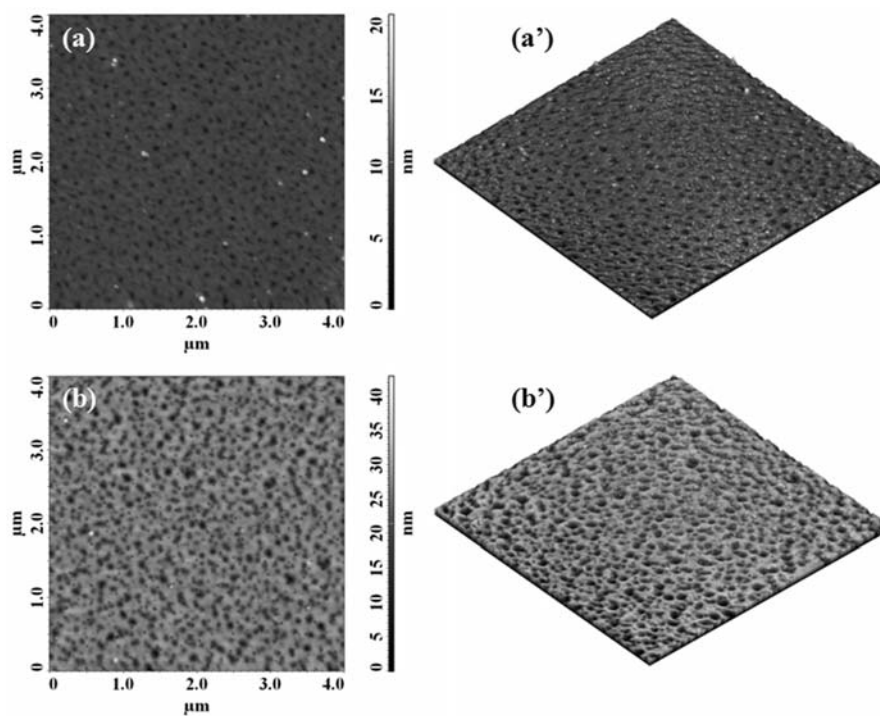
Fig. 3 – Normalized UV-Vis absorption spectra of **PF** and **PFc** in thin films.

Table 2

Roughness parameters and pore characteristics collected from  $1 \times 1 \mu\text{m}^2$  AFM images of **PF** and **PFc** polymer films

Samples	Roughness parameters			Pore characteristics	
	Ha (nm)	Sq (nm)	Sdr (%)	Number of pores	$D_{\text{average}}^a$ (nm)
<b>PF</b>	4.3	1.1	0.28	89	$24.5 \pm 11.7$
<b>PFc</b>	20.5	2.8	0.92	30	$33.0 \pm 22.1$

<sup>a</sup> Average diameter.Fig. 4 – The 2D and 3D height AFM images of **PF** (a, a') and **PFc** (b, b').

In order to evaluate the topography of the **PF** and **PFc** polymer film surfaces AFM experiments were also performed, shown in Fig. 4 and summarized in Table 2. They afforded the roughness parameters as the average height ( $H_a$ ), root mean square roughness of the formations ( $S_q$ ) as well as surface area ratio ( $S_{dr}$ ), pore characteristics, see Table 2.

The 2D height AFM images on the top surface of **PF** (a) and **PFc** (b) copolymer films are shown in Fig. 4 (a, b). The scanning area of  $1 \times 1 \mu\text{m}^2$  of the films prepared by spin-coating from a THF solution, on glass slides, without drying, reveals that both samples showed a terraced morphology with the single-molecule steps in certain regions indicating that, the molecules are likely to be edge-on and tilted.<sup>19</sup>

The terraced morphology gives to the surface a porous aspect, with various pore size and two dimensional ordered structures.

## EXPERIMENTAL

9,9-dioctylfluorene-2,7-bis(trimethyleneborate) (**1**), 2,7-dibromofluorene-9-one, tetrakis(triphenylphosphine) palladium (0) [Pd(PPh<sub>3</sub>)<sub>4</sub>], dimethylformamide (DMF), were purchased from (Sigma-Aldrich) and used as received. Malononitrile (Merck) were used without further purification, and all other solvents were analytical grade and used as received. The general synthetic procedures for monomers and copolymers synthesis was previously reported.<sup>18</sup>

## CHARACTERIZATION

Polymer analyses were performed by <sup>1</sup>H-NMR spectrometry (Bruker Advance 400 MHz, in CD<sub>2</sub>Cl<sub>2</sub>). FT-IR analyses of the powder polymers were performed in a Specord Carl Zeiss Jena FTIR spectrophotometer. UV-Vis absorption and fluorescence emission spectra were measured in thin films on a Specord 200 and a Perkin Elmer LS55 spectrophotometer, respectively. The surface profile of the polymeric films was evaluated by atomic force microscopy (AFM). AFM measurements were performed in air, at room temperature, in the tapping mode using a Scanning Probe Microscope with commercially available NSG10 cantilever (Solver PRO-M, NTMDT, Russia). Films of copolymers were prepared by spin-coating from dilute CH<sub>3</sub>Cl solutions at 3000 rpm for 60 s on a WS-400B-6NPP-Lite Single Wafer Spin Processor (Laurel Technologies Corporation, USA).

## CONCLUSIONS

In summary, new random conjugated polyrotaxane consisting of 9-dicyanomethylene fluorene inclusion complex in  $\gamma$ CD (electron-accepting) and methyltriphenylamine (electron-donating) moieties have been incorporated into 9,9-dioctylfluorene units by randomly copolymerization, designed and successfully synthesized. The rotaxane copolymer is more hydrophilic than the non-complexed homologue and the presence of  $\gamma$ CD induces the increase of the solubility in polar solvents, the absorption intensity and improves the surface characteristics. The next step in our studies is to develop further aspects of this material for optical applications.

*Acknowledgements:* This work was supported by a grant of the Roumanian National Authority for Scientific Research, CNCS – UEFISCDI, project no PN-II-ID-PCE-2011-3-0035.

## REFERENCES

1. Y. K. Fang, C. L. Liu, C. Li, C. J. Lin, R. Mezzenga and W. C. Chen, *Adv. Funct. Mater.*, **2010**, *20*, 3012-3024.
2. W.-H. Chen, K.-L. Wang, W.-Y. Hung, W.-I. Hung, J.-C. Jiang, D.-J. Liaw, K.-R. Lee, J.-Y. Lai and C.-L. Chen, *J. Polym. Sci. Part A: Polym. Chem.*, **2010**, *48*, 4654-4667.
3. Z. Jiang, W. Zhang, H. Yao, C. Yang, Y. Cao, J. Qin, G. Yu and Y. Liu, *J. Polym. Sci. Part A: Polym. Chem.*, **2009**, *47*, 3651-3661.
4. U. Scherf and E. J. W. List, *Adv. Mater.*, **2002**, *14*, 477-487.
5. A. Babel and S. A. Jenekhe, *Macromolecules*, **2003**, *36*, 7759-7764.
6. M. G. Manjunatha, A. V. Adhikari and P. K. Hedge, *Eur. Polym. J.*, **2009**, *45*, 763-771.
7. C. H. Kuo, W. K. Cheng, K. R. Lin, M. K. Leung and K. H. Hsieh, *J. Polym. Sci. Part A: Polym. Chem.*, **2007**, *45*, 4504-4513.
8. I. F. Perepichka, A. F. Popov, T. V. Orekhova, M. R. Btyce, A. M. Andrievskii, A. S. Batsanov, J. A. K. Howard and N. I. Sokolov, *J. Org. Chem.*, **2000**, *65*, 3053-3063.
9. W.-Y. Wong, K.-H. Choi, G.-L. Lu and J.-Y. Shi, *Macromol. Rapid Commun.*, **2001**, *22*, 461-465.
10. A. Farcas, N. Jarroux, P. Guegan, A. Fifere, M. Pinteala and V. Harabagiu, *J. Appl. Polym. Sci.*, **2008**, *110*, 2384-2392.
11. A. Farcas, I. Ghosh, N. Jarroux, V. Harabagiu, P. Guegan and W. M. Nau, *Chem. Phys. Lett.*, **2008**, *465*, 96-101.
12. A. Farcas, N. Jarroux, I. Ghosh, P. Guegan, W. M. Nau and V. Harabagiu, *Macromol. Chem. Phys.*, **2009**, *210*, 1440-1449.
13. A. Farcas, N. Jarroux, V. Harabagiu and P. Guegan, *Eur. Polym. J.*, **2009**, *45*, 795-803.
14. A. Farcas, I. Ghosh, V. C. Grigoras, I. Stoica, C. Peptu and W. M. Nau, *Macromol. Chem. Phys.*, **2011**, *212*, 1022-1031.

15. A. Farcas, I. Stoica, A. Stefanache, C. Peptu, F. Farcas, N. Marangoci, L. Sacarescu, V. Harabagiu and P. Guégan, *Chem. Phys. Lett.*, **2011**, *508*, 111-116.
16. A. Farcas, I. Ghosh and W. M. Nau, *Chem. Phys. Lett.*, **2012**, *535*, 120-125.
17. A. Farcas, A.-M. Resmerita, A. Stefanache, M. Balan and V. Harabagiu, *Beilstein J. Org. Chem.*, **2012**, *8*, 1505-1514.
18. A. Farcas, S. Janietz, V. Harabagiu, P. Guegan and P.-H. Aubert, *J. Polym. Sci. Part A: Polym. Chem.*, **2013**, *51*, 1672-1683.
19. L. Zalewski, S. Broveli, M. Bonini, J. M. Mativetsky, M. Wykes, E. Orgiu, T. Breiner, M. Kastler, F. Dötz, F. Meinardi, H. L. Anderson, D. Beljonne, F. Caciali and P. Samori, *Adv. Funct. Mater.*, **2011**, *21*, 834-844.